Multifrequency mismatch functions for nonlinear parametric identifications

Thierry Scotti, Armand Wirgin

7 - 12 SEPTEMBER 2014, KRAKÓW
FORUM ACUSTICUM

Multifrequency mismatch functions for nonlinear parametric identifications

Thierry Scotti
LMA, CNRS, UPR 7051, Aix-Marseille Univ, Centrale Marseille, F-13402 Marseille Cedex20, France.

Armand Wirgin
LMA, CNRS, UPR 7051, Aix-Marseille Univ, Centrale Marseille, F-13402 Marseille Cedex20, France.

Summary
This investigation is concerned with the ill-posed nature of (non-linear) inverse problems, in the frequency domain, for which the unknown parameters are determined, in iterative manner, by seeking the minima of a mismatch function quantifying the discrepancy between given data and the output of a numerical model. One might think that the identification can be done solely by the search of the minima of the mismatch function, but this problem is mathematically ill-posed and it is illusory to try to identify a satisfactory solution until the problems of stability (noisy data) and non-uniqueness (local minima) are resolved. This paper shows that a mismatch function resulting from summing up mono frequency mismatch functions corresponding to several different frequencies turns the inverse problem into a global optimization problem and overcomes the problem of the sensitivity of solutions to noisy data, without requiring a priori information on the probed medium.

PACS no. 43.20.+g, 02.30.Zz

1. Introduction

Parametric imaging - or more generally inverse parametric identification - is often performed through linearization of the governing equations (wave-interaction model) so as to express the unknowns (i.e., the unknown parameters of the inverse problem) as a function of the data (given measured fields). The solution is then determined through simplifications and approximations and therefore does not completely reflect reality. On the contrary, our interest is to make no linearization or higher order approximation and therefore the solution(s) cannot be expressed as a linear function of the data [1] - hence the term "nonlinear". The method is to search, in iterative manner, for the set of unknown parameters that minimize the discrepancy (i.e., the measure of which is a cost or an objective/mismatch function) between given data (i.e., measurements) and the output of a numerical model (retrieval model). This procedure requires solving a forward problem at each step of the iterative process.

One might think that the identification can be done solely by the search of the minima of the mismatch function. But this problem is mathematically ill-posed [2]: the solution may not exist, is not unique (the mismatch function presents local minima) and does not depend continuously on the data (a small perturbation of data gives rise to important perturbations of the solution). Whatever the precision with which the forward problem is solved during the inversion and whatever the chosen optimization scheme, it is illusory to try to identify a satisfactory solution, until the problem of stability and non-uniqueness is resolved.

It has become fairly common, if enough a priori information is available, that the use of a weight-penalized mismatch function can circumvent the ill-posed nature of the problem. This consists in adding to the mismatch function a weighted penalty term: $\delta \mid \mathcal{L} \mid$ where $\mathcal{L}$ is a particular operator and δ the associated weight term [3, 4]. One drawback of this approach is the choice of the $\mathcal{L}$ and the associated weighted term δ remains difficult and must involving a priori information on the target - often some information about the smoothness of the solution [5, 6, 7]. The solution then depends strongly on these choices and turns out to be "art" insofar as a bad choice leads to false identifications.

Based on what was observed in a particular case, [8]: 1/ the location of the minima of the mono-frequency mismatch functions change when the wavenumber of the probe radiation changes, and 2/ the least-affected minimum correspond to the sought-for solution [9], a multifrequency-mismatch-function was constructed which allows one to overcome the problems of local minima [10].

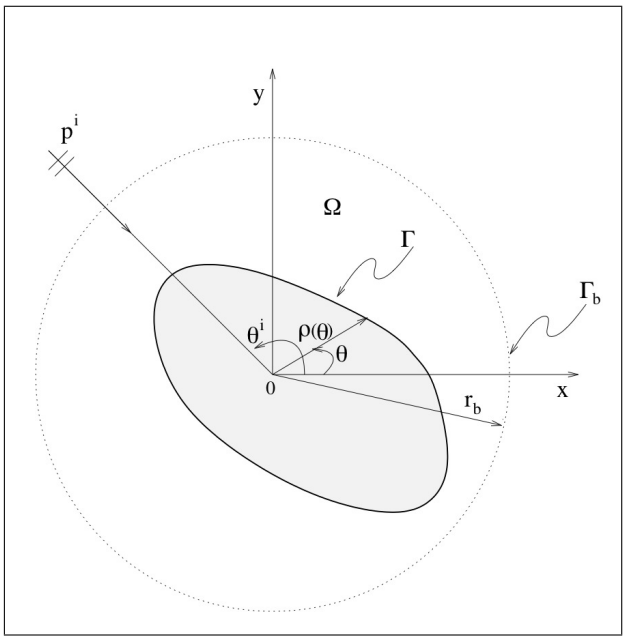

Figure 1. Scattering configuration.

This paper is more particularly dedicated to the problem of stability of the solutions with respect to noisy measurements. Through an example of a 2D parameter reconstruction of the boundary of a target we find that the multifrequency mismatch function increases the stability of solutions with respect to data noise, without requiring any a priori information on the target or of the probed medium. The principles of the proposed approach can easily be extended to other kinds of parameter reconstructions: material properties, source location, ...

2. Problem ingredients

2.1. Scattering configuration

We assume that the bounded (in its cross-section plane) cylindrical target (i.e., body) is filled with a non-penetrable fluid-like medium and is embedded in an unbounded space filled with a (well-characterized) linear, homogeneous, isotropic, non-absorbing fluid-like medium (Ω) (Figure (1)). The boundary (Γ) of the body is assumed to be representable by the parametric equation $r = \rho(\theta)$ where$0 \leq \theta < 2\pi$, and ρ is a single-valued continuous function of θ in the prescribed interval. The incident monochromatic field is that of a plane longitudinal wave ($p^i = \exp(i\mathbf{k}\cdot\mathbf{x})$, $\mathbf{k}$ being the incident wave-vector and $\mathbf{x} = (x, y) = (r, \theta)$) the vector position of the point $\mathbf{x}$. The time-dependence ($\exp(-i\omega t)$),with ω the angular frequency and t the time) is implicit in this as well as in succeeding field variables. The origin O in the $(Oxyz)$ Cartesian coordinate system is assumed (for convenience) to be located within the target. The essential task in the forward scattering context is to determine p^d via the governing equations:

$$(\Delta + k^2)p(\mathbf{x},\omega) = 0 \ ; \ \mathbf{x} \in \Omega \ , \tag{1}$$

$$p^d(\mathbf{x},\omega) = p(\mathbf{x},\omega) - p^i(\mathbf{x},\omega) \ ; \ \mathbf{x} \in \Omega, \tag{2}$$

$$p^i(r,\theta,k) = \exp\left(-ikr\cos(\theta - \theta^i)\right), \tag{3}$$

$$p(\mathbf{x},\omega) = 0 \ ; \ \mathbf{x} \in \Gamma \ , \tag{4}$$

$$\lim_{r\to\infty} r^{1/2}(\partial_r - ik_0)p^d(\mathbf{x},\omega) = 0 \ ; \ \forall\theta \in [0, 2\pi] \tag{5}$$

2.2. Field representation

A complete family of generally non-orthogonal functions representation of the scattered field is employed: the so-called partial wave representation [11] as an exact expression in $\Omega^+ = \{r > \bar{r}; 0 < \theta < 2\pi\}$ with $\bar{r} = \max_{0<\theta<2\pi}\rho(\theta)$:

$$p(k,r,\theta) = p^i(r,\theta) + \sum_{n=-\infty}^{\infty} a_n H_n^{(1)}(kr)e^{in\theta} \tag{6}$$

J_n and $H_n^{(1)}$ are respectively the n-th order Bessel and Hankel function of the first kind. Numerically speaking the series are truncated to $2N + 1$ terms.

3. Forward problems

The general *forward scattering problem* is: given the incident wave-field, as well as the frequency, the material properties of the host medium Ω, the characteristics of the target (material properties, location, and shape), compute the (total) wave-field on a virtual cylinder (whose boundary is) Γ_b enclosing the body whose radius is $r_b > \bar{r} = \max_{0<\theta<2\pi}\rho(\theta)$.

3.1. Measurement simulations

Since we do not dispose of real data, the measurements of the diffracted field on Γ_b are numerically generated by the Rayleigh method [12, 13]. Introducing the field representation Eq.(6) into the boundary condition Eq.(4) and projecting onto the Fourier base $\{\exp(-im\theta) \, ; \, m = -N, ..., 0, ..., N\}$, leads to a linear system of equation that enables the determination of the coefficients a_n (Eq.(6)):

$$\mathcal{H}\mathcal{A} = \mathcal{D} \tag{7}$$

with, $m = -N, ..., N; n = -N, ..., N$ and,

$$\mathcal{H} = H_{mn} = \int_0^{2\pi} H_n^{(1)}(k_0\rho(\theta))e^{i(n-m)\theta} \ d\theta \tag{8}$$

$$\mathcal{D} = D_m = -\int_0^{2\pi} p^i(\rho(\theta),\theta)e^{-im\theta} \ d\theta \tag{9}$$

$$\mathcal{A} = A_n = a_n. \tag{10}$$

3.2. Physical model for the inversion

During the inversion the forward problem will be solved using a "retrieval model" which appeals to the Intersecting Canonical Body Approximation (ICBA) [14]. This approximation consists in assuming, for a particular scattering direction θ, that the response of the actual body to the incident wave at any point (r, θ) can be approximated by the response of the circular cylinder whose radius is equal to the local radius of the real body $\rho(\theta)$ in the aforementioned scattering direction. In other words, for a given angle of observation θ, the coefficients in the partial wave representation of the scattered field Eq.(6) are those (b_n) of the circular cylinder having the same local radius (η) - at this angle of observation - as that of the real body $\rho(\theta)$:

$$p(k, r_b, \theta) \approx \tilde{p}(\eta \mid k, r_b, \theta) \tag{11}$$

with $\tilde{p}(\eta \mid r_b, \theta, k)$ the field diffracted by the circular cylinder of radius $\eta = \rho(\theta)$. More precisely,

$$\tilde{p}(\eta \mid k, r_b, \theta) = p^i(r, \theta, k) + ... \\ ... + \sum_{n=-\infty}^{\infty} b_n(\eta) H_n^{(1)}(kr) e^{in\theta} \tag{12}$$

with

$$\eta = \rho(\theta), \tag{13}$$

and

$$b_n(\eta) = -(-i)^n \frac{J_n(k\eta)}{H_n^{(1)}(k\eta)} \exp(-in\theta^i). \tag{14}$$

4. Inverse problem

The *inverse scattering problem* can be formulated as follows: given the incident wavefield, as well as the frequency, the material properties of the host medium Ω, the wavefield on the circular boundary of a virtual cylinder Γ_b enclosing the body whose radius is $r_b > \bar{r} = \max_{0<\theta<2\pi} \rho(\theta)$, reconstruct the (location and) shape parameters (set of vector lengths joining the origin O to the point $(\rho(\theta), \theta)$ on the surface) of the scattering body.

4.1. Basic form of the mismatch function

As concerns the inverse problem employing the ICBA retrieval model [15, 16], given a measurement point r_b, θ on Γ_b, the expression of the mismatch function $\mathcal{F}$ is:

$$\mathcal{F}(\eta \mid k, r_b, \theta) = \Big| p(k, r_b, \theta)^{\text{"measured"}} - ... \\ ... - \tilde{p}(\eta \mid k, r_b, \theta) \Big|^{\alpha}, \tag{15}$$

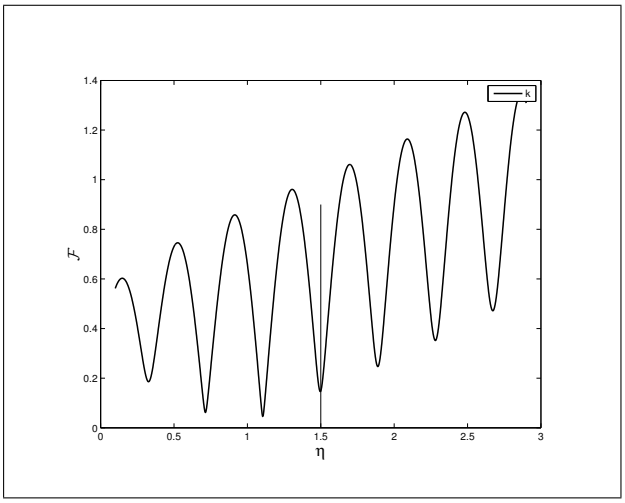

Figure 2. see Eq.(15)) for $k = 8$, $\theta = \pi$, $r_b = 3$, the target is an ellipsoid of semi-axis $(1.0 - 1.5)$. One can observe the presence of local minima: the expected solution $(\eta = 1.5)$ is not the global one $(\eta = 1.1)$. The vertical straight line indicates the expected location of the solution.

for some chosen value of α, with $\tilde{p}(\eta \mid k, r_b, \theta)$ given by Eq.(12).

The inversion then reduces to: 1/ matching, for any particular scattering direction θ, the expression of $\tilde{p}$ with the "given" data $p^{\text{"measured"}}$, 2/ finding, for this scattering direction, the set of the trial shape parameters $\mathbb{S} = \{\eta_l \ ; = 1, ...L\}$ for which the mismatch function Eq.(15) admits a minimum and 3/ identifying the "correct" minimum (one particular value among the set $\mathbb{S}$) and associate it with the local radius $\rho(\theta)$ of the (unknown) object for this particular direction. If this is done for a set of measurements in an angular sector (or all around the body) then the discretized form of the shape function is thereby partially (or totally) obtained.

One might think that the identification can be done solely by the search of the minima of the mismatch function. But this problem is mathematically ill-posed: the solution is not unique (presence of local minima, as seen in Fig. (2) , and does not depend continuously on the data, as seen in Fig. (3). of globally [17].

4.2. Multifrequency mismatch function: local minima

To overcome the problem of local minima, a first approach was published in [8, 9]. From an asymptotic analysis of the cost function equation (Eq.15), it was shown that, from a mathematical point of view, the use of measurements of the response of a target (circular cylinder) to two monochromatic probe plane waves having different frequencies enables a non-ambiguous identification of the boundary (radius) of the scattering body among all local minima. The method is based on the fact that the locations of the minima of the mono-frequency mismatch function change when

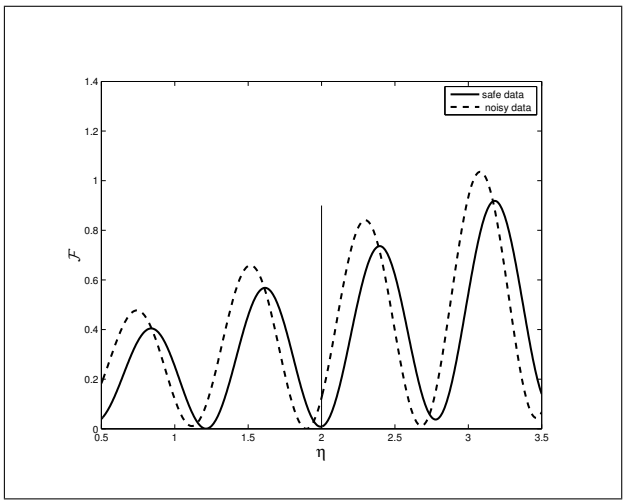

Figure 3. see Eq.(15)) for $k = 4$, $\theta = \pi$, $r_b = 6$, the target is an ellipsoid of semi-axis $(1.5 - 2)$. One can observe the displacements of the locations of the minima when adding noise to the data. The vertical straight line indicates the expected location of the solution.

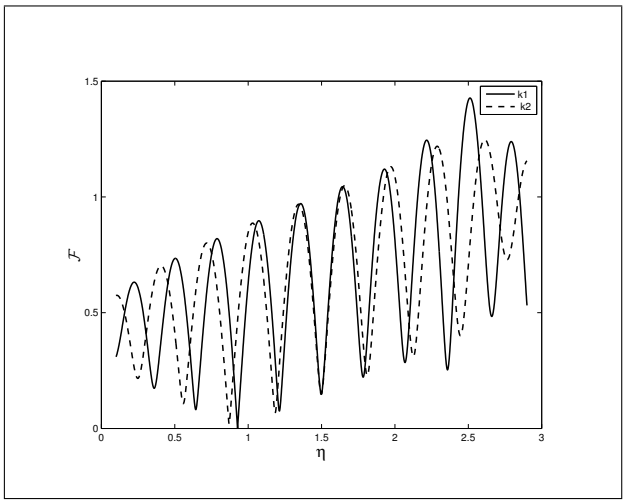

Figure 4. Mono-frequency mismatch functions $\mathcal{F}$ (see Eq.(15)) for $k_1 = 10$ and $k_2 = 11$, $\theta = \pi$, the target is an ellipsoid of semi-axis $(1.0 - 1.5)$. On can observe that the only minimum location that doesn't change when the frequency of the mismatch function change is the expected solution ($\rho = 1.5$ in this case).

the wavenumber of the probe radiation changes and that the least-affected minimum corresponds to the sought-for solution. Hence the idea to compare the location of the minima of two mismatch functions, corresponding to the target being probed at two different frequencies, and select the least-affected one. An illustration of this principle is shown in Figure(4): : one can observe that the location of the minima of the mono-frequency mismatch function changes when the wavenumber of the probe radiation changes except for the sought-for solution.

Based on the above observations, a second approach was proposed in [10]. Rather than selecting the minimum that moves less when changing the frequency (which is not a trivial numerical task because one must determine all the minima in a given range and then compare each couple of values), it was proposed to build an "objective" function $\hat{\mathcal{F}}$ (named hereafter multifrequency mismatch function) consisting of the sum of the mono-frequency mismatch functions $\mathcal{F}$ of Eq.(15) in a given range of frequencies: $\mathcal{K} = \{k_m; m = 1, ..., M\}$

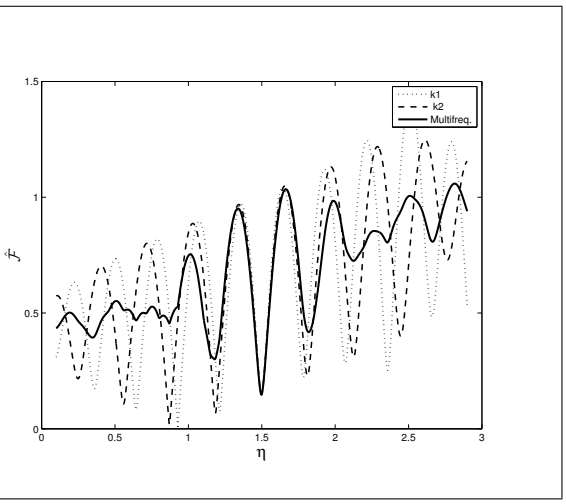

Figure 5. Same as Figure(4) but the plot of the multifrequency cost function is added (see Eq.(16): M=4, $k_1 = 8, k_2 = 9, k_3 = 10, k_4 = 11$). One observes that the "multifrequency" cost function admits a global minimum at the expected position ($\rho = 1.5$).

$$\hat{\mathcal{F}}(\eta \mid \mathcal{K}, r_b, \theta^l) = \frac{1}{M} \sum_{m=1}^{M} \Big| p(k_m, r_b, \theta)^{\text{"measured"}} - ... \\ ... - \tilde{p}(\eta \mid k_m, r_b, \theta) \Big|^{\alpha}, \quad (16)$$

In Figure(5) one can observe that the multi-frequency cost function has a global minimum corresponding to the expected solution.

4.3. Multifrequency mismatch function: noisy data

The second point we want to stress concerns the behavior of the reconstructed parameters when the data is noisy. "Measurements" with additive stochastic noise were simulated in the following manner. Let u and v be the real and imaginary parts of a perfect measured field variable w (which is a function of the polar angle θ). Let U and V be the real and imaginary parts of the corresponding noisy field variable W. We generated W from w, at every measurement angle, by means of

$$U = u + (\phi_u - 0.5) \mid \max_{\theta \in [0,2\pi[} u - \min_{\theta \in [0,2\pi[} u \mid p_n/100, \\ V = v + (\phi_v - 0.5) \mid \max_{\theta \in [0,2\pi[} v - \min_{\theta \in [0,2\pi[} v \mid p_n/100 \quad (17)$$

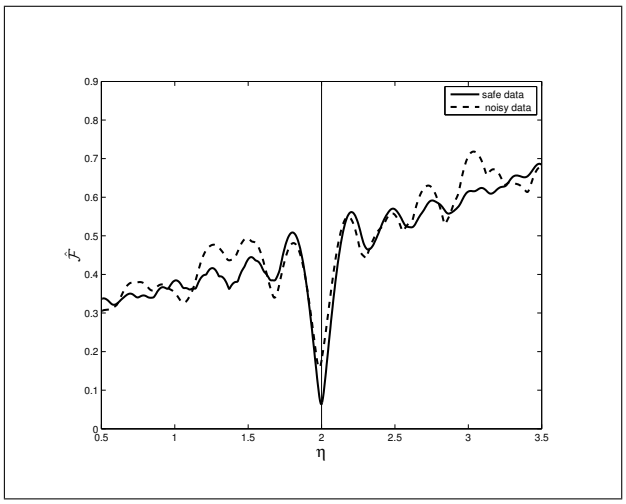

Figure 6. Multi-frequency mismatch functions (M=4, $k_1 = 8, k_2 = 9, k_3 = 10, k_4 = 11$). One can observe that the impact of noisy data is minimized with respect of the mono-frequency approach. (Figure(3)).

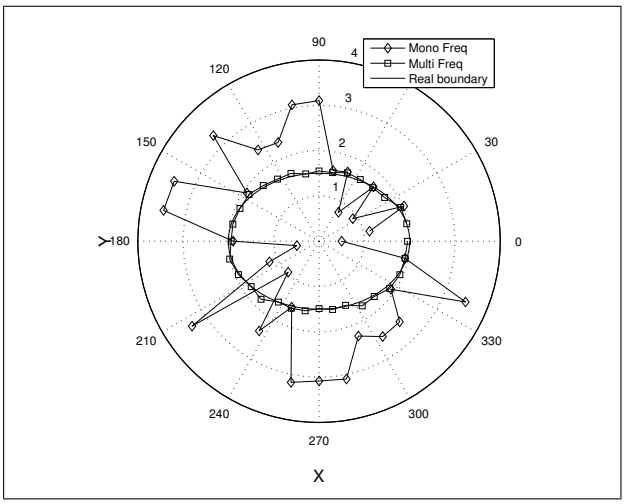

Figure 7. Comparison of the boundary reconstructions of an ellipsoid of semi-axis (1.5-2.0) with the multifrequency and mono-frequency mismatch functions in presence of noisy data.

where ϕ_u and ϕ_v are two (statistically unrelated) numbers located in the interval [0, 1] and p_n is the percentage noise (ranging from 0 to 100).
One observes in Figure(6), that the location of the global minimum of the multifrequency mismatch function is more accurate (with respect of the expected value, see the vertical straight line) than what is obtained by the mono frequency mismatch function (Figure(3)). Various configurations and values of p_n, M, and k_n were chosen, with always the same observation: in the case of noisy data, the multifrequency mismatch function always enables a more accurate identification than the mono-frequency mismatch function.

5. Numerical applications: boundary reconstruction of a target in presence of noisy data

The last step is to perform the procedure for a complete boundary reconstruction in the presence of noisy data. The procedure is described in §4.1 with only one change: the "expected" minimum is now chosen to be the global minimum of the multifrequency mismatch function. The mono-frequency mismatch function is computed for $k = 4$ while the multifrequency mismatch function is computed for $k_1 = 1, k_2 = 2, k_3 = 3, k_4 = 4$. The noisy parameter (see Eq.(17)) is $p_n = 80$. Result is shown in Figure(7): the boundary reconstruction obtained via the mono-frequency mismatch function presents many artifacts (due to noisy data and ?), in contrast with the boundary obtained via the location of the global minimum of the multifrequency mismatch function.

6. Conclusion

When it is not possible to express the unknown of the inverse problem in the form of a (linear) function of the data because the linearization of the wave-interaction problem is not possible - or desired, nonlinear inversions are faced the problem of the presence of local minima and high sensitivity of the solution to small variations of the data. The ill-posed nature of the problem is generally bypassed by using a weight-penalized mismatch function that requires a priori information on the (unknown) target, thus making the solution very dependent on the choices associated with the penalization (a bad choice leads to incorrect identifications).

Starting from an initial mathematical result [8] [9], we find, via a series of numerical simulations, that a mismatch function resulting from the sum of the mono-frequency mismatch functions (without any regularization or penalty term) for several (arbitrarily- chosen) frequencies, enables: 1/ the unambiguous location and reconstruction of the boundary of a target, and 2/ far less sensitivity of the inversion to noisy "measurements" (even if they are actually numerically simulated).

References

[1] R.L. Parker: Understanding inverse theory, Ann. Rev. Earth Planet. Sci. (**5**) (1977), pp. 35-64.

[2] D. Colton and R. Kress: Inverse acoustic and electromagnetic scattering theory. Springer applied mathematical sciences, 1992, Berlin.

[3] A. Tikhonov and V. Arsnine: Methodes de Resolution de Problemes Mal Poses. 1974, Editions MIR, Moscow.

[4] C.R. Vogel, Computational Methods for Inverse Problems, SIAM, 2002.

[5] L. Horesh and E. Haber: Sensitivity computation of the $l1$ minimization problem and its application to dictionary design of ill-posed problems. Inverse Problems, **25**(9), 2009.

[6] A. Tarantola and B. Valette: Generalized nonlinear inverse problems solved using the least squares criterion. Reviews of Geophysics and Space Physics, **20**(2), 1982, pp. 219-232.

[7] H. Engl and P. Kugler: Nonlinear inverse problems: Theoretical aspects and some industrial applications. In Multidisciplinary Methods for Analysis Optimization and Control of Complex Systems, B. et al, ed., **6**, 2005, Springer Berlin Heidelberg, pp. 3-47.

[8] E. Ogam and T. Scotti and A. Wirgin: Non-ambiguous boundary identification of a cylindrical object by acoustic waves, Comptes Rendus de l'Académie des Sciences - Series IIB - Mechanics 329, (**1**) (2001), pp. 61 - 66.

[9] E. Ogam and T. Scotti and A. Wirgin: Reduction of the ambiguity of shape reconstruction of cylindrical bodies using both real and synthetic acoustic scattering data, in Acoustics, Mechanics and the Related Topics of Mathematical Analysis (World Scientific, Singapore, 2002), pp. 222-228.

[10] L. Le Marrec and P. Lasaygues and T. Scotti and C. Tsogka, "Efficient Shape Reconstruction of Non-Circular Tubes Using Broadband Acoustic Measurements", Acta Acustica united with Acustica 92 (2006), pp. 355-361(**7**)).

[11] A. Wirgin and T. Scotti: Complete family of functions methods, based on the Rayleigh hypothesis and on the extinction theorem, for inverse acoustic wave scattering problems. Acustica-Acta Acustica **84** (1998), 1083-1090.

[12] P. M. Van Den Berg and J. T. Fokkema: The Rayleigh hypothesis in the theory of diffraction by a cylindrical obstacle, IEEE Trans. Anten. Prop. (**2**) (1979), pp. 577-583.

[13] Bolomey, J.C. and Wirgin, A.: Numerical comparison of the Green's function and the Waterman and Rayleigh theories of scattering from a cylinder with arbitrary cross-section, Electrical Engineers, Proceedings of the Institution of 121, (**8**) (1974), pp. 794 -804.

[14] A. Wirgin and T. Scotti: Wide-band approximation of the sound field scattered by an impenetrable body of arbitrary shape, Journal of Sound and Vibration 194, (**4**) (1996), pp. 537 - 572.

[15] T. Scotti and A. Wirgin: Location and shape reconstruction of a soft body by means of canonical solutions and measured scattered sound fields, Comptes Rendus de l'Académie des Sciences - Series IIB - Mechanics-Physics-Chemistry-Astronomy 320, (**12**) (1995), pp. 641-646.

[16] T. Scotti and A. Wirgin: Shape reconstruction of an impenetrable scattering body via the Rayleigh hypothesis, Inverse Problems (**12**) (1996), pp. 1027–1055.

[17] Scotti, T. and Wirgin, A.: Location and Shape Reconstruction Via Diffracted Waves and Canonical Solutions,in Acoustical Imaging, (**22**), Tortoli, Piero and Masotti, Leonard eds, Springer US, pp 101-106